

Clinical significance of tumor-infiltrating immune cells focusing on BTLA and Cbl-b in patients with gallbladder cancer

Seiji Oguro,^{1,2,3,4} Yoshinori Ino,¹ Kazuaki Shimada,³ Yutaka Hatanaka,^{5,6} Yoshihiro Matsuno,^{5,6} Minoru Esaki,³ Satoshi Nara,³ Yoji Kishi,³ Tomoo Kosuge^{3,4} and Nobuyoshi Hiraoka^{1,2}

¹Division of Molecular Pathology, National Cancer Center Research Institute, Tokyo; ²Divisions of Pathology and Clinical Laboratories; ³Hepatobiliary and Pancreatic Surgery Division, National Cancer Center Hospital, Tokyo; ⁴Advanced Clinical Research of Cancer, Juntendo University Graduate School of Medicine, Tokyo; ⁵Department of Surgical Pathology; ⁶Research Division of Companion Diagnostics, Hokkaido University Hospital, Sapporo, Japan

Key words

Anergy, BTLA, gallbladder cancer, immune checkpoint, immune microenvironment

Correspondence

Nobuyoshi Hiraoka, Division of Pathology and Clinical Laboratories, National Cancer Center Hospital, 5-1-1 Tsukiji, Chuo-ku, Tokyo 104-0045, Japan.
Tel.: +81-3-3542-2511; Fax: +81-3-3543-5073;
E-mail: nhiraoka@ncc.go.jp

Funding Information

Ministry of Education, Culture, Sports, Science and Technology of Japan, Japan Society for the Promotion of Science ('KAKENHI 25460486'), National Cancer Center Research and Development Fund.

Received July 15, 2015; Revised September 16, 2015;
Accepted September 18, 2015

Cancer Sci 106 (2015) 1750–1760

doi: 10.1111/cas.12825

The host immune system plays a significant role in tumor control, although most cancers escape immune surveillance through a variety of mechanisms. The aim of the present study was to evaluate the clinicopathological significance of a novel co-inhibitory receptor, B and T lymphocyte attenuator (BTLA), the anergy cell marker Casitas-B-lineage lymphoma protein-b (Cbl-b), and clinical implications of tumor-infiltrating immune cells in gallbladder cancer (GBC) tissues. We investigated 211 cases of GBC, 21 cases of chronic cholecystitis (CC), and 11 cases of xanthogranulomatous cholecystitis (XGC) using immunohistochemistry to detect tissue-infiltrating immune cells and their expression of BTLA and Cbl-b, and carried out correlation and survival analyses. The density of infiltrating T cells was significantly higher in CC and XGC than in GBC. The density ratio of BTLA⁺ cells to CD8⁺ T cells (BTLA/CD8) and that of Cbl-b⁺ cells to CD8⁺ T cells (Cbl-b/CD8) were significantly higher in GBC than in CC and XGC. The FOXP3/CD4, BTLA/CD8, and Cbl-b/CD8 ratios were significantly correlated with each other, and also with malignant phenotypes. Survival analyses revealed that a lower density of tumor-infiltrating CD8⁺ cells, and higher Foxp3/CD4, BTLA/CD8, and Cbl-b/CD8 ratios were significantly associated with shorter overall survival and disease-free survival in GBC patients. Multivariate analyses showed that M factor, perineural invasion, BTLA/CD8, and Cbl-b/CD8 were closely associated with shorter overall survival. These findings suggest that higher ratios of BTLA/CD8 and Cbl-b/CD8 are independent indicators of unfavorable outcome in GBC patients, and that upregulation of BTLA in cancer tissues is involved in inhibition of antitumor immunity.

Gallbladder cancer (GBC) is the most common malignant biliary neoplasm and the seventh most common gastrointestinal cancer.⁽¹⁾ Complete surgical resection is the standard treatment for patients with localized disease, and the only potentially definitive curative therapy.^(2,3) However, because most cases of GBC are diagnosed at an advanced stage, when the disease is not amenable to surgical resection, this malignancy is highly lethal, with a 5-year survival rate of <5% for such patients.^(4,5) Therefore, a more thorough understanding of GBC is essential for the development of new therapeutic strategies.

Based on a growing body of evidence from both animal and human models, it is generally accepted that naturally occurring immunity can play a significant role in the control of tumor development and progression.⁽⁶⁾ Most clinically evident cancers exhibit immune escape, where the cancer microenvironment can induce immune tolerance through a variety of mechanisms, such as the production of soluble immunosuppressive factors and the recruitment of suppressor immune cells.^(7,8) Elucidation of the molecular and cellular events

responsible for tumor immune escape is essential in order to make anticancer therapy truly effective in a clinical setting.⁽⁹⁾ Tumor-infiltrating immune cells are one of the representative cellular components of host antitumor immune responses and tumor immune escape. Tumor-infiltrating immune cells are composed of different cell subsets, which determine the overall protumor or antitumor characteristics. For example, a high proportion of CD8⁺ T cells infiltrating the cancer tissue can be a favorable prognostic indicator in colorectal,^(10,11) ovarian,⁽¹²⁾ esophageal,⁽¹³⁾ liver,⁽¹⁴⁾ and pancreatic^(15,16) cancers. In contrast, patients whose cancers show marked infiltration of regulatory T cells tend to have a poorer prognosis in several types of cancer.^(17–19) Two groups have studied the tumor-infiltrating immune cells in GBC using small numbers of cases (45 cases⁽²⁰⁾ and 69 cases⁽²¹⁾), and showed that tumor-infiltrating CD8⁺ T cells and CD4⁺ T cells were indicators of favorable prognosis, whereas tumor-infiltrating FOXP3⁺ cells or CD20⁺ B cells had no significant impact on outcome.

In addition to immunosuppressive cells, tumor cells deploy distinct mechanisms to evade immune attack, including

expression of ligands for co-inhibitory receptors on T cells.⁽²²⁾ Recently, the distinct role of co-inhibitory receptors, such as CTL-associated protein 4 (CTLA-4) and programmed cell death 1 (PD-1), in this process has been extensively investigated.⁽²³⁾ The function of antigen-specific CD8⁺ T cells, which may protect against both infectious and malignant diseases, can be impaired by ligation of these inhibitory receptors. Expression of these receptors has been linked to functional impairment of T cells in cancer, and therapeutic blockade of these two pathways has shown clinical promise. Antagonist antibodies have been developed in order to overcome immune evasion, and anti-CTLA-4 and anti-PD1 antibodies have been tested in clinical trials with encouraging results.^(24–27) Anti-CTLA4 antibody was the first agent shown to confer a survival benefit on patients with advanced melanoma, and was approved by the US FDA in 2010.

B and T lymphocyte attenuator (BTLA) has been identified as a novel co-inhibitory receptor, expressed by a majority of lymphocytes, and shows structural and functional similar-

ties to CTLA-4 and PD-1.⁽²⁸⁾ Because tumor-infiltrating immune cells express multiple co-inhibitory receptors, it is assumed that dual or triple blockade of co-inhibitory receptors will enhance antitumor immunity. Indeed, combined blockade of the PD-1/programmed death-ligand 1 (PD-L1) and CTLA-4 pathways, and that of the PD-1/PD-L1 and lymphocyte activation gene 3 (LAG3) pathways, has been shown to enhance antitumor effects in a human clinical study and animal model studies.^(29–31) Thus, BTLA is expected to be a new target for interventions aimed at reversal of immune evasion and boosting of antitumor immunity in cancer patients. Expression of BTLA has been reported in B-cell small lymphocytic lymphoma/chronic lymphocytic leukemia cells and gastric cancer cells.^(32,33) However, there are currently no data on the immunohistochemical expression of BTLA in the microenvironment of human tumors, and the clinical significance of BTLA expression in tumor-infiltrating immune cells remains to be identified. It has also been reported that BTLA plays a critical role in the induction of peripheral T cell anergy *in vivo*.⁽³⁴⁾ T cell anergy is also widely accepted as an impor-

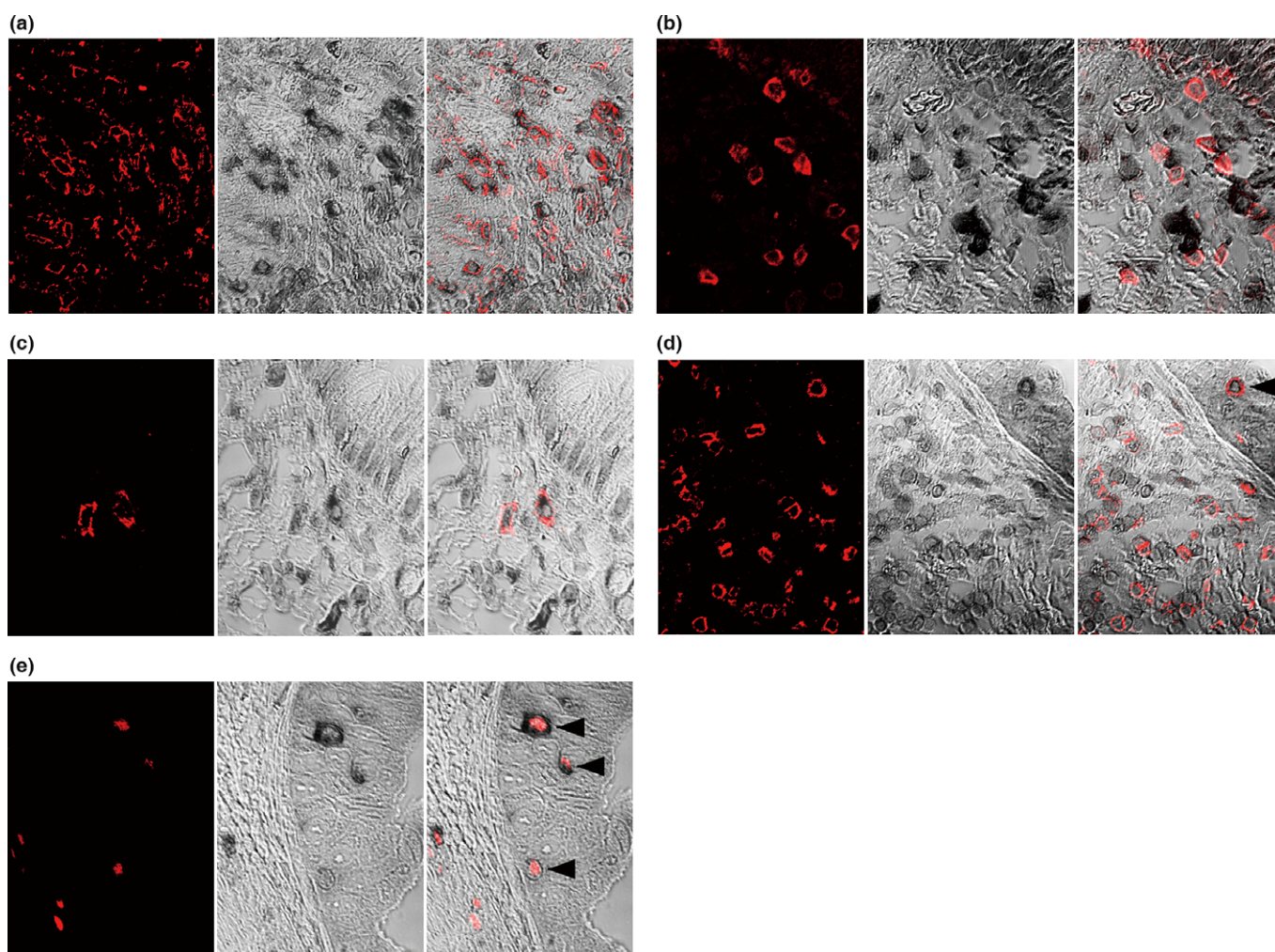


Fig. 1. Double immunostaining features in gallbladder cancer samples. (a) Most B and T lymphocyte attenuator (BTLA)⁺ cells (black) are CD4⁺ T cells (red). (b, c) BTLA (black) staining is sometimes present in CD8⁺ T cells (red) (b) or CD1a⁺ (red) dendritic cells infiltrated in the cancer stroma (c). (d) Tumor-infiltrating CD8⁺ T cells (red) are often Casitas-B-lineage lymphoma protein-b (Cbl-b)⁺ (black). CD8⁺ T cells that have infiltrated and become attached to cancer cells (arrowhead) are Cbl-b⁺ anergic cells. (e) FOXP3⁺ regulatory T cells (red) often express Cbl-b (black). Arrowheads indicate regulatory T cells that have infiltrated and become attached to cancer cells. (a–e) Left column shows immunofluorescence staining for CD4 (a), CD8 (b, d), CD1a (c), or FOXP3 (e). Center column shows immunohistochemical staining for BTLA (a–c) or Cbl-b (d, e). Right column shows merged images of left and center photographs.

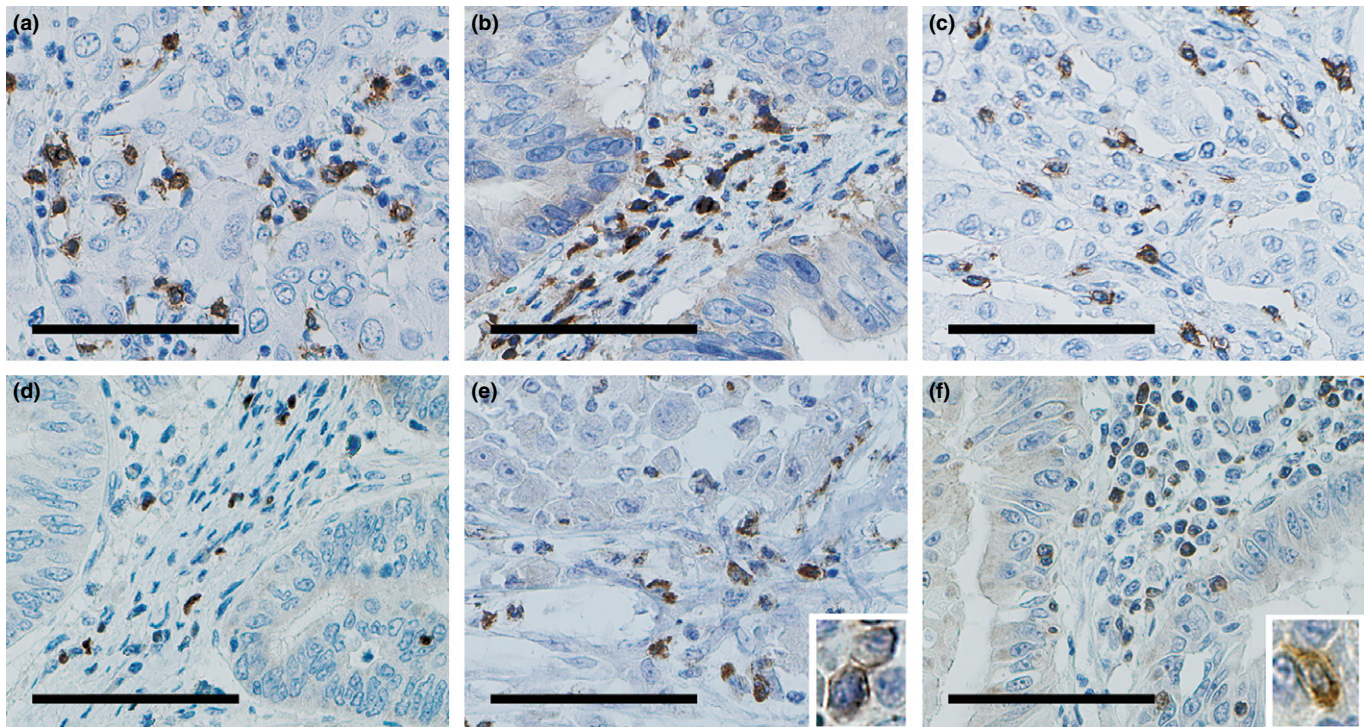


Fig. 2. Immunohistochemical features of tumor-infiltrating cells. These representative photos show: (a) CD3⁺ T cells, (b) CD4⁺ T cells, (c) CD8⁺ T cells, (d) FOXP3⁺ T cells, (e) B and T lymphocyte attenuator (BTLA)⁺ cells, and (f) Casitas-B-lineage lymphoma protein-b (Cbl-b)⁺ cells. Scale bar = 100 μ m. High power views are shown in insets of (e) and (f).

tant mechanism of tumor immune escape,⁽³⁵⁾ although no previous studies have shown anergy cells in tissues. Casitas-B-lineage lymphoma protein-b (Cbl-b), an E3 ubiquitin ligase, is critical for establishing the threshold for T cell activation and for induction of T cell anergy.^(36,37)

The aim of this study was to evaluate the clinicopathological impact of BTLA as well as the clinical implications of tumor-infiltrating immune cells in patients with GBC to assess their potential as new targets for cancer immunotherapy.

Materials and Methods

Study population. Clinical and pathologic data and the specimens used for immunohistochemical analysis were obtained through a detailed retrospective review of the medical records of all 211 patients with GBC who had undergone surgical resection between 1985 and 2012 at the National Cancer Center Hospital (Tokyo, Japan). All of the patients included in this study underwent macroscopic curative resection, and all had primary carcinomas of the gallbladder. Neuroendocrine neoplasms were excluded. The median follow-up period was 28 months (range, 1–289 months) for the patients overall: 89 patients (42.2%) were alive, 84 (39.8%) had died because of GBC, and 38 (18.0%) had died of other causes. During the study period, adjuvant chemotherapy was not carried out. In addition, we analyzed cases of chronic cholecystitis (CC) ($n = 21$) and xanthogranulomatous cholecystitis (XGC) ($n = 11$) as controls for evaluating the significance of tumor-infiltrating immune cells.

This study was approved by the Institutional Review Board of the National Cancer Center, Japan. Informed consent was obtained from all participants involved in the study, and all

clinical investigations were carried out in line with the principles of the Declaration of Helsinki.

Pathological examination. All of the carcinomas were examined pathologically and classified according to the World Health Organization classification,⁽³⁸⁾ Union for International Cancer Control TNM classification,⁽³⁹⁾ and the Japanese Society of Biliary Surgery classification of biliary tract carcinoma.⁽⁴⁰⁾ Tumors were staged and the histopathologic variables (histopathological grading, lymphatic, venous, and perineural invasion) were evaluated and described in accordance with their classifications.^(39,40)

Immunohistochemistry. Immunohistochemistry was carried out on formalin-fixed, paraffin-embedded tissue sections using the avidin-biotin complex method as described previously.⁽⁴¹⁾ We used 4- μ m-thick serial sections of representative blocks with antibodies against the following: CD3 (PS1; 1:100) from Santa Cruz Biotechnology (Santa Cruz, CA, USA), CD4 (368; 1:100) and CD8 (4B11; 1:200) from Leica Microsystems (Newcastle-upon-Tyne, UK), FOXP3 (42; 1:100) produced in house,⁽¹⁸⁾ BTLA (HPA047211; 1:500) from Atlas Antibodies (Stockholm, Sweden), and Cbl-b (246C5A; 1:50) from Abcam (Cambridge, UK). Immunohistochemistry without the primary antibody was used as a negative control.

Double immunostaining. We carried out double staining on formalin-fixed paraffin-embedded sections. First, the 4- μ m-thick sections were immunostained using anti-BTLA antibody or anti-Cbl-b antibody as the primary antibody, and visualized with 3,3'-diaminobenzidine. After the tissue sections had been treated with glycine-HCl (pH 2.5), they were subjected to immunofluorescence staining using antibodies against each of the following antigens: CD1a (O10, Lab Vision, Fremont, CA, USA), CD3, CD4, CD8, CD14 (7, Leica Microsystems), CD20

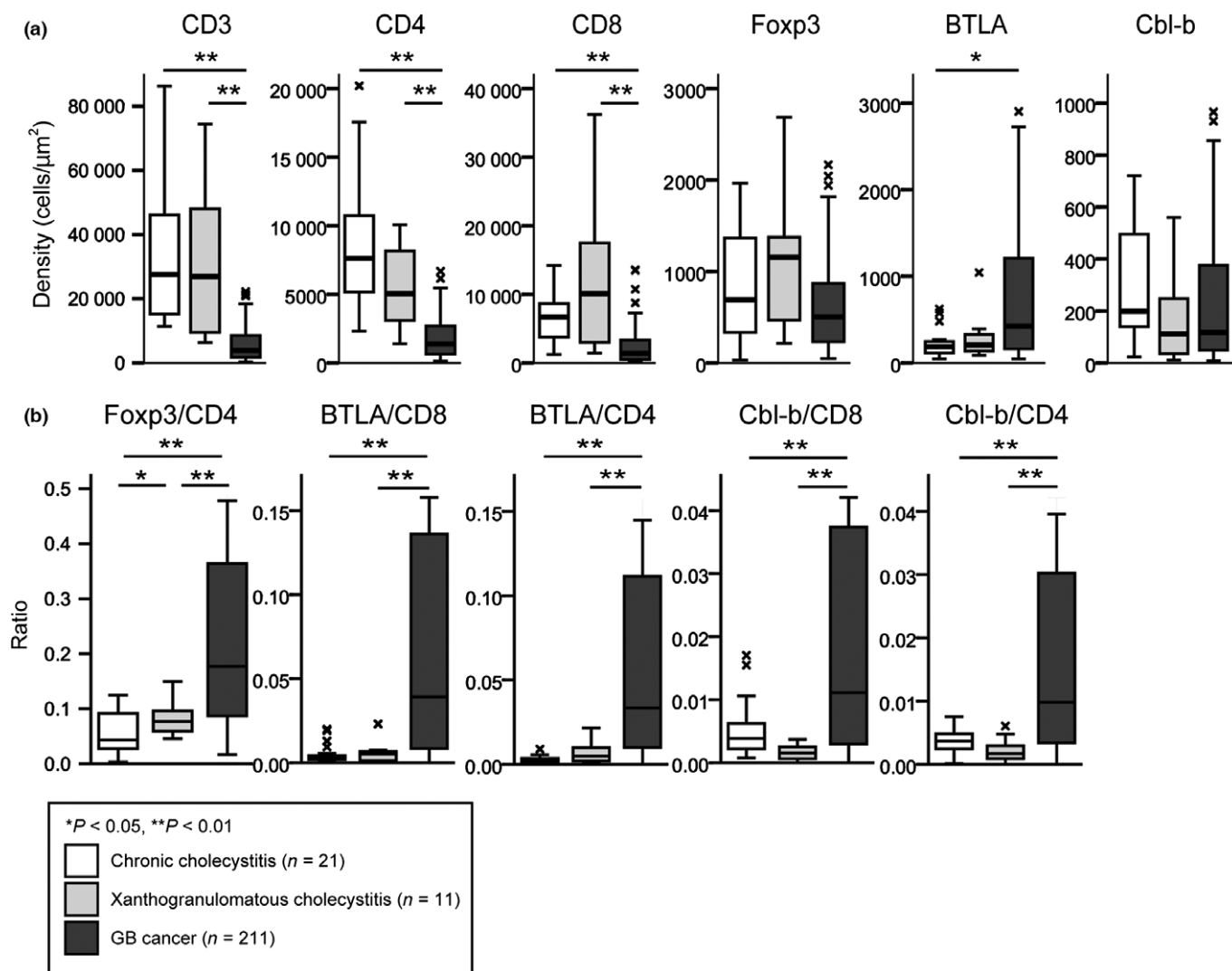


Fig. 3. Comparison of cells infiltrating into chronic cholecystitis (CC, $n = 21$), xanthogranulomatous cholecystitis (XGC, $n = 11$), and gallbladder cancer (GBC, $n = 211$). (a) Density of immunolabeled T cells (cells/ μm^2). (b) Density ratio of FOXP3⁺ cells to CD4⁺ T cells (FOXP3/CD4), that of B and T lymphocyte attenuator (BTLA)⁺ cells to CD8⁺ T cells (BTLA/CD8), that of BTLA⁺ cells to CD4⁺ T cells (BTLA/CD4), that of Casitas-B-lineage lymphoma protein-b (Cbl-b)⁺ cells to CD8⁺ T cells (Cbl-b/CD8), and that of Cbl-b⁺ cells to CD4⁺ T cells (Cbl-b/CD4). The line in the middle of the boxes shows the median value. The bottom and top of the box indicates the 25th and 75th percentiles, respectively. The T-bars that extend from the boxes show inner fences and "x" indicates outliers. Significant values were * $P < 0.05$ and ** $P < 0.01$.

(L26, DAKO), CD56 (1B6, Leica Microsystems), CD68 (KP1, DAKO), CD207 (12D6, Leica Microsystems), CD208 (104.G4, Immunotech, Fullerton, CA, USA), FOXP3, BTLA, and Cbl-b. Immunostained tissue sections were analyzed with a confocal microscope (LSM5 Pascal; Carl Zeiss, Jena, Germany) equipped with a 15-mW Kr/Ar laser.

Quantitative evaluation of tumor-infiltrating T cell subsets, BTLA-positive cells, and Cbl-b-positive cells. After immunohistochemistry, the microscopic images were imported as digital photo files using a NanoZoomer Digital Pathology system (Hamamatsu Photonics, Hamamatsu, Japan), and the density of the immunolabeled cells was analyzed using the image analysis software, Tissue Studio (Definiens, Munich, Germany). We manually selected one area as region of interest (ROI), in which the CD3-labeled T cells had infiltrated into the tumor most densely in the specimen, when we checked it in low-power view. In each individual case, the same ROI was applied to all the other immunostained images. The immunola-

beled cells inside the ROI were automatically counted on the basis of staining intensity. In each analysis we confirmed that the immunohistochemically positive lymphocytes were appropriately detected. The density of positive cells was calculated by dividing their number by the ROI area (cells/ μm^2). Also, we calculated the density ratio of FOXP3 to CD4 (FOXP3/CD4), that of BTLA to CD3 or CD8 (BTLA/CD3, BTLA/CD8), and that of Cbl-b to CD3 or CD8 (Cbl-b/CD3, Cbl-b/CD8). For survival and correlation analyses, patients were divided into two groups showing high and low cell infiltration, using the median value as a cut-off.

Statistical analysis. We expressed continuous data as median and range and compared them using the Mann-Whitney U -test. We compared categorical data by Pearson's χ^2 or Fisher's exact test, as appropriate. We constructed survival curves by the Kaplan-Meier method and compared them using the log-rank test. We calculated the length of overall survival (OS) from the date of surgical resection to the date

Table 1. Interrelationships between clinicopathological variables and tumor-infiltrating cells

Variables	CD3			CD4			CD8			FOXP3			FOXP3/CD4		
	Low	High	<i>P</i> -value	Low	High	<i>P</i> -value	Low	High	<i>P</i> -value	Low	High	<i>P</i> -value	Low	High	<i>P</i> -value
Age, years			0.302			0.033			0.063			0.016			0.837
<68 (<i>n</i> = 105)	56	49		60	45		59	46		61	44		53	52	
≥68 (<i>n</i> = 106)	49	57		45	61		46	60		44	62		52	54	
Gender			0.046			0.948			0.833			0.002			0.537
Female (<i>n</i> = 100)	57	43		50	50		49	51		61	39		52	48	
Male (<i>n</i> = 111)	48	63		55	56		56	55		44	67		53	58	
Tumor main location			0.308			0.009			0.422			0.681			0.025
Gf, Gb (<i>n</i> = 104, 46)	78	72		66	84		72	78		76	74		82	68	
Gn, C (<i>n</i> = 40, 21)	27	34		39	22		33	28		29	32		23	38	
T			0.538			0.295			0.060			0.951			0.023
1, 2 (<i>n</i> = 28, 66)	49	45		43	51		40	54		47	47		55	39	
3, 4 (<i>n</i> = 74, 43)	56	61		62	55		65	52		58	59		50	67	
N			0.836			0.448			0.448			0.063			0.033
0 (<i>n</i> = 107)	54	53		56	51		56	51		60	47		61	46	
1 (<i>n</i> = 104)	51	53		49	55		49	55		45	59		44	60	
M			0.963			0.522			0.126			0.398			0.009
0 (<i>n</i> = 145)	72	73		70	75		67	78		75	70		81	64	
1 (<i>n</i> = 66)	33	33		35	31		38	28		30	36		24	42	
Histopathological grading			0.303			0.239			0.727			0.063			0.003
1 (<i>n</i> = 99)	53	46		45	54		48	51		56	43		60	39	
2, 3, 4 (<i>n</i> = 62, 45, 5)	52	60		60	52		57	55		49	63		45	67	
Lymphatic invasion			0.016			0.352			0.962			0.069			0.128
0 (<i>n</i> = 68)	42	26		37	31		34	34		40	28		39	29	
1 (<i>n</i> = 143)	63	80		68	75		71	72		65	78		66	77	
Venous invasion			0.010			0.537			0.436			0.083			0.022
0 (<i>n</i> = 88)	53	35		46	42		41	47		50	38		52	36	
1 (<i>n</i> = 123)	52	71		59	64		64	59		55	68		53	70	
Perineural invasion			0.148			0.442			0.295			0.372			0.002
0 (<i>n</i> = 94)	52	42		44	50		43	51		50	44		58	36	
1 (<i>n</i> = 117)	53	64		61	56		62	55		55	62		47	70	
CD3						<0.001			<0.001			<0.001			0.005
Low (<i>n</i> = 105)				77	28		74	31		71	34		42	63	
High (<i>n</i> = 106)				28	78		31	75		34	72		63	43	
CD4									<0.001			<0.001			<0.001
Low (<i>n</i> = 105)							81	24		70	35		29	76	
High (<i>n</i> = 106)							24	82		35	71		76	30	
CD8												<0.001			<0.001
Low (<i>n</i> = 105)										71	34		37	68	
High (<i>n</i> = 106)										34	72		68	38	
FOXP3															0.001
Low (<i>n</i> = 105)													64	41	
High (<i>n</i> = 106)													41	65	
FOXP3/CD4															
Low (<i>n</i> = 105)															
High (<i>n</i> = 106)															
BTLA															
Low (<i>n</i> = 105)															
High (<i>n</i> = 106)															
BTLA/CD8															
Low (<i>n</i> = 105)															
High (<i>n</i> = 106)															
BTLA/CD4															
Low (<i>n</i> = 105)															
High (<i>n</i> = 106)															
Cbl-b															
Low (<i>n</i> = 105)															
High (<i>n</i> = 106)															
Cbl-b/CD8															
Low (<i>n</i> = 105)															
High (<i>n</i> = 106)															

Density ratios are shown of FOXP3 to CD4 (FOXP3/CD4), B and T lymphocyte attenuator (BTLA) to CD8 (BTLA/CD8), BTLA to CD4 (BTLA/CD4), Casitas-B-lineage lymphoma protein-b (Cbl-b) to CD8 (Cbl-b/CD8), and Cbl-b to CD4 (Cbl-b/CD4). Bold values, *P* < 0.05; underlined values, positively correlated. C, cystic duct; Gb, gallbladder body; Gf, gallbladder fundus; Gn, gallbladder neck.

BTLA			BTLA/CD8			BTLA/CD4			Cbl-b			Cbl-b/CD8			Cbl-b/CD4		
Low	High	P-value	Low	High	P-value	Low	High	P-value	Low	High	P-value	Low	High	P-value	Low	High	P-value
		0.046			0.242			0.046			0.630			0.302			0.535
45	60		48	57		45	60		54	51		49	56		50	55	
60	46		57	49		60	46		51	55		57	49		55	51	
		0.948			0.627			0.733			0.046			0.627			0.085
50	50		48	52		51	49		57	43		52	48		56	44	
55	56		57	54		54	57		48	63		54	57		49	62	
		0.158			0.617			0.845			0.422			0.158			0.025
70	80		73	77		74	76		72	78		80	70		82	68	
35	26		32	29		31	30		33	28		26	35		23	38	
		0.023			<0.001			0.005			0.372			0.003			0.011
55	39		62	32		57	37		50	44		58	36		56	38	
50	67		43	74		48	69		55	62		48	69		49	68	
		0.007			0.113			0.301			0.113			0.946			0.190
63	44		59	48		57	50		59	48		54	53		58	49	
42	62		46	58		48	56		46	58		52	52		47	57	
		0.083			0.003			0.020			0.802			0.034			0.009
78	67		82	63		80	65		73	72		80	65		81	64	
27	39		23	43		25	41		32	34		26	40		24	42	
		0.063			0.033			0.033			0.632			0.146			0.191
56	43		57	42		57	42		51	48		55	44		54	45	
49	63		48	64		48	64		54	58		51	61		51	61	
		0.035			0.069			0.128			0.128			0.403			0.128
41	27		40	28		39	29		39	29		37	31		39	29	
64	79		65	78		66	77		66	77		69	74		66	77	
		0.083			0.022			0.146			0.146			0.058			0.022
50	38		52	36		49	39		49	39		51	37		52	36	
55	68		53	70		56	67		56	67		55	68		53	70	
		0.735			0.045			0.372			0.951			0.110			0.023
48	46		54	40		50	44		47	47		53	41		55	39	
57	60		51	66		55	62		58	59		53	64		50	67	
		0.063			0.046			0.002			0.063			0.302			0.046
59	46		45	60		41	64		59	46		49	56		45	60	
46	60		60	45		64	42		46	60		57	49		60	46	
		0.007			0.011			<0.001			<0.001			0.003			<0.001
62	43		43	62		35	70		67	38		42	63		37	68	
43	63		62	44		70	36		38	68		64	42		68	38	
		0.630			<0.001			<0.001			0.016			<0.001			0.001
54	51		29	76		37	68		61	44		32	73		40	65	
51	55		76	30		68	38		44	62		74	32		65	41	
		<0.001			0.945			0.837			0.001			0.449			0.837
68	37		52	53		53	52		64	41		50	55		53	52	
37	69		53	53		52	54		41	65		56	50		52	54	
		0.063			<0.001			<0.001			0.837			<0.001			<0.001
59	46		69	36		75	30		53	52		68	37		74	31	
46	60		36	70		30	76		52	54		39	67		31	75	
					<0.001			<0.001			<0.001			<0.001			0.016
			80	25		78	27		69	36		67	38		61	44	
			25	81		27	79		36	70		39	67		44	62	
								<0.001			0.007			<0.001			<0.001
						88	17		62	43		80	25		70	35	
						17	89		43	63		26	80		35	71	
											0.033			<0.001			<0.001
									60	45		73	32		73	32	
									45	61		33	73		32	74	
														<0.001			<0.001
												76	29		75	30	
												30	76		30	76	
																	<0.001
															90	16	
															15	90	

of death from any cause, calculated the length of disease-free survival (DFS) from the date of surgical resection to the date of the first radiologic findings for recurrence, and censored those on the date of the last follow-up. To evaluate the prognostic significance of tumor-infiltrating lymphocytes and cells expressing inhibitory molecules in patients with GBC, univariate and multivariate Cox analyses were applied. The factors found to be significant by univariate analysis were subjected to multivariate analysis. $P < 0.05$ was considered to denote statistical significance for all analyses. Statistical analyses were carried out using spss version 20.0 (SPSS, Chicago, IL, USA).

Results

Immunophenotype of BTLA⁺ cells and Cbl-b⁺ cells. To examine the immunophenotype of BTLA⁺ cells and Cbl-b⁺ cells, double immunostaining was carried out (Fig. 1). BTLA was present in a proportion of CD3⁺ T cells, CD4⁺ T cells, CD8⁺ T cells, CD20⁺ B cells, CD14⁺ monocytes, CD68⁺ macrophages, CD1a⁺ dendritic cells (DCs), CD207⁺ DCs, or CD208⁺ DCs, although the majority of BTLA⁺ cells were CD4⁺. In contrast, no expression of BTLA was found in FOXP3⁺ cells, CD56⁺ natural killer (NK) cells, or Cbl-b⁺ cells. Cbl-b was expressed in a small proportion of CD3⁺ T cells, CD4⁺ T cells, CD8⁺ T cells, Foxp3⁺ cells, and CD20⁺ B cells, and was not expressed in CD56⁺ NK cells, CD14⁺ monocytes, CD68⁺ macrophages, or DCs. There were no BTLA⁺Cbl-b⁺ cells in the cancer tissues, although T cells that had infiltrated into cancer cell nests and become attached to cancer cells were often positive for Cbl-b, and sometimes for BTLA. No tumor cells expressed BTLA or Cbl-b in our series.

Infiltration of T cell subsets, BTLA⁺ cells, and Cbl-b⁺ cells. The median area of the ROI was 10 129 950 μm^2 among the 212 cases of GBC, 1 336 266 μm^2 among the 21 cases of CC, and 4 922 487 μm^2 among the 11 cases of XGC. Representative photos of each type of positive cell are shown in Figure 2. Although there were too few samples of normal gallbladder tissue to compare with cancer tissue statistically, we found several CD3⁺ cells, CD4⁺ cells, and CD8⁺ cells in lamina propria. And a few FOXP3⁺ cells or Cbl-b⁺ cells but no BTLA⁺ cells were found. Figure 3(a) shows a comparison of T cell subsets, BTLA-positive cells, and Cbl-b-positive cells infiltrating into CC ($n = 21$), XGC ($n = 11$), and GBC ($n = 211$). The density of CD3⁺ cells, CD4⁺ cells, and CD8⁺ cells in CC and XGC was significantly higher than that in GBC, respectively ($P < 0.01$). In contrast, the density of FOXP3⁺ cells, BTLA⁺ cells, and Cbl-b⁺ cells did not differ significantly among the diseases, except for the density of BTLA⁺ cells between CC and GBC. The number of suppressor cells such as regulatory T cells (Tregs) is often affected by the entire T cell infiltration.^(16,18) It is often better to estimate the immune microenvironment from the ratio of the number of tumor-infiltrating suppressor cells to that of the immune responsive cell population, rather than the absolute number of tumor-infiltrating suppressor cells.^(16,18,42) We used the ratio of FOXP3 density to CD4 density (FOXP3/CD4), the ratio of BTLA density to CD8 density (BTLA/CD8), and the ratio of Cbl-b density to CD8 density (Cbl-b/CD8); comparisons of these ratios between the diseases are depicted in Figure 3(b). FOXP3/CD4, BTLA/CD8, and Cbl-b/CD8 in GBC were significantly higher than those in CC and XGC, respectively ($P < 0.01$). Comparisons of the BTLA/CD3 and Cbl-b/CD3 ratios among

GBC, CC, and XGC showed similar profiles to those of BTLA/CD8 and Cbl-b/CD8, respectively (Fig. S1).

Interrelationships between clinicopathological variables and tumor-infiltrating cells. We analyzed the interrelationships between clinicopathological variables of GBC and tumor-infiltrating T cell subsets, BTLA⁺ cells, and Cbl-b⁺ cells (Table 1). FOXP3/CD4, BTLA/CD8, and Cbl-b/CD8 showed significant and positive correlations with each other. FOXP3/CD4 was significantly correlated with most of the conventional clinicopathological variables: tumor main location, T factor, N factor, M factor, histopathological grading, venous invasion, and perineural invasion. Likewise, BTLA/CD8 was significantly correlated with T factor, M factor, histopathological grading, venous invasion, and perineural invasion, and Cbl-b/CD8 was significantly correlated with T factor and M factor. The interrelationships of BTLA/CD3 and Cbl-b/CD3 with various factors were similar to those of BTLA/CD8 and Cbl-b/CD8, respectively (data not shown).

Prognostic significance of tumor-infiltrating T cell subsets, BTLA⁺ cells, and Cbl-b⁺ cells. Kaplan–Meier survival analyses revealed that a lower density of tumor-infiltrating CD8⁺ T cells, and higher FOXP3/CD4, BTLA/CD8, and Cbl-b/CD8 ratios were significantly associated with both shorter OS and DFS in GBC patients (Fig. 4). Higher BTLA/CD3 and Cbl-b/CD3 ratios were closely associated with both shorter OS and DFS (Fig. S2). Five-year survival rate, median survival time, and Cox analyses in the groups categorized by each of the parameters of tumor-infiltrating cells and the conventional clinicopathological variables are summarized in Tables 2 and S1. When the variables that had been found to be significant by univariate analysis were subjected to multivariate analysis, M factor, perineural invasion, BTLA/CD8, and Cbl-b/CD8 were closely associated with shorter OS. In addition, T factor, M factor, perineural invasion, and Cbl-b/CD8 were significantly associated with shorter DFS.

Discussion

Here we evaluated for the first time the clinical impact of BTLA in cancer tissues. First, we assessed whether tumor-infiltrating immune cells reflected the character of the tumor immune microenvironment, as it has been reported in various other cancers. The present study, including 211 cases of GBC, revealed that greater infiltration of CD8⁺ T cells and CD4⁺ T cells in the cancer tissue was a favorable prognostic indicator, as has been reported for many other cancers and for GBC.^(20,21) It also showed that a higher prevalence of Tregs (FOXP3/CD4) was significantly correlated with malignant phenotypes and an unfavorable outcome, suggesting that Tregs play a role in controlling the immune response to GBC. Furthermore, a higher ratio of Cbl-b⁺ anergic lymphocytes to CD8⁺ T cells (or to total T cells) was significantly correlated with advanced T factor, distant metastasis, and poorer prognosis. Therefore, the importance of antitumor immunity, represented by tumor-infiltrating immune cells, in the outcome and control of cancer was confirmed for GBC.

Tumor cells are able to evade immune recognition and destruction through a variety of mechanisms. One such mechanism is the immunosuppressive action of co-inhibitory molecules.⁽²³⁾ BTLA is a co-inhibitory molecule whose expression has been reported in mice and human blood cells. However, no previous study has investigated the expression of BTLA in the microenvironment of human tumors. Here, we found that BTLA was expressed on a proportion of several different types

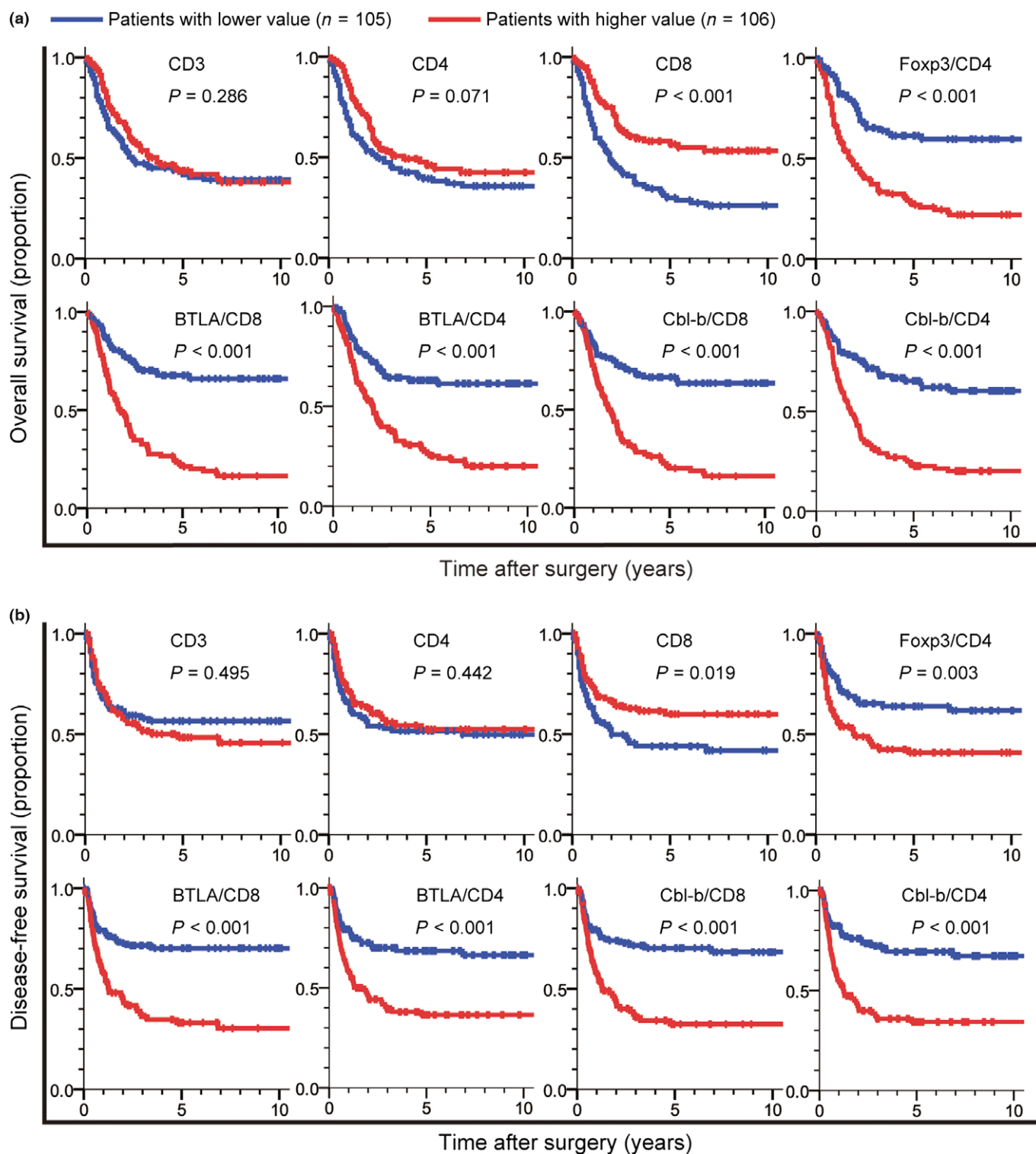


Fig. 4. Kaplan–Meier survival curves comparing (a) overall survival and (b) disease-free survival in gallbladder cancer patients between the high (red) and low (blue) value groups with regard to the density of tumor-infiltrating CD3⁺ T cells, CD4⁺ T cells, CD8⁺ T cells and the density ratio of the FOXP3⁺ T cells to CD4⁺ T cells (Foxp3/CD4), that of B and T lymphocyte attenuator (BTLA)⁺ cells to CD8⁺ T cells (BTLA/CD8), that of BTLA⁺ cells to CD4⁺ T cells (BTLA/CD4), that of Casitas-B-lineage lymphoma protein-b (Cbl-b)⁺ cells to CD8⁺ T cells (Cbl-b/CD8), and that of Cbl-b⁺ cells to CD4⁺ T cells (Cbl-b/CD4). *P*-values were obtained by log-rank test.

of tumor-infiltrating immune cells, including CD3⁺ T cells, CD4⁺ T cells, CD8⁺ T cells, CD20⁺ B cells, CD14⁺ monocytes, CD68⁺ macrophages, CD1a⁺ DCs, CD207⁺ DCs, and CD208⁺ DCs. Our clinicopathological investigation revealed

that BTLA/CD8 was increased in malignant disease (GBC) relative to benign disease (CC and XGC) and that the BTLA/CD8 ratio in tumor-infiltrating immune cells was enhanced in patients with more advanced cancer. Furthermore, a higher

Table 2. Univariate and multivariate analyses for variables associated with overall survival (OS) and disease-free survival (DFS) in patients with gallbladder cancer

Variables	Category	n	5-year survival, %	Median survival time, months	OS				DFS							
					Univariate		Multivariate		Univariate		Multivariate					
					HR	95%CI	P-value	HR	95%CI	P-value	HR	95%CI	P-value	HR	95%CI	P-value
Age ≥68 years	No./yes	105/106	40.8/44.5	34.1/38.2	0.958	0.669	1.371	0.813	1.024	0.679	1.545	0.910				
Gender	F/M	100/111	47.6/38.1	56.1/27.8	1.308	0.911	1.876	0.145	1.395	0.915	2.127	0.122				
Location	Gf,Gb/ Gn,C	104,46/40,21	48.4/29.6	54.6/27.1	1.422	0.973	2.078	0.069	1.667	1.092	2.543	0.018				
T	1,2,3,4	28,66/74,43	71.5/19.2	215.2/17.8	4.587	3.013	6.986	<0.001	7.453	4.255	13.055	<0.001	2.906	1.431	5.898	0.003
N	0/1	107/104	58.3/25.8	215.2/19.5	2.713	1.870	3.937	<0.001	3.868	2.467	6.064	<0.001	3.325	1.631	6.779	0.001
M	0/1	145/66	54.7/15.1	138.8/12.9	3.772	2.607	5.457	<0.001	2.156	1.462	3.179	<0.001	2.318	1.493	3.598	<0.001
Grading	1/2,3,4	99/62,45,5	61.5/26.1	215.2/19.5	3.071	2.049	4.535	<0.001	3.659	2.303	5.814	<0.001	3.325	1.631	6.779	0.001
L	0/1	68/143	71.7/27.9	215.2/22.9	3.500	2.195	5.581	<0.001	5.737	3.042	10.818	<0.001	3.325	1.631	6.779	0.001
V	0/1	88/123	69.4/22.3	215.2/19.8	3.861	2.505	5.814	<0.001	4.984	2.956	8.404	<0.001	3.325	1.631	6.779	0.001
Pn	0/1	94/117	71.7/18.7	215.2/17.2	4.715	3.093	7.187	<0.001	3.833	2.453	5.989	<0.001	3.325	1.631	6.779	0.001
CD3	Low/high	105/106	41.5/43.7	29.4/43.6	0.824	0.576	1.179	0.291	1.152	0.762	1.742	0.501	2.906	1.431	5.898	0.003
CD4	Low/high	105/106	39.3/46.0	29.7/46.4	0.721	0.503	1.033	0.075	0.853	0.565	1.287	0.448	3.325	1.631	6.779	0.001
CD8	Low/high	105/106	30.0/56.6	22.9/191.0	0.478	0.331	0.691	<0.001	0.616	0.406	0.933	0.022	3.325	1.631	6.779	0.001
Foxp3/CD4	Low/high	105/106	61.1/26.8	NR/20.8	2.783	1.894	4.088	<0.001	1.855	1.217	2.826	0.004	3.325	1.631	6.779	0.001
BTLA/CD8	Low/high	105/106	65.8/20.0	191.0/20.8	3.577	2.387	5.359	<0.001	2.154	1.400	3.313	<0.001	3.325	1.631	6.779	0.001
BTLA/CD4	Low/high	105/106	63.0/25.2	NR/24.6	2.892	1.957	4.274	<0.001	2.362	1.530	3.648	<0.001	3.325	1.631	6.779	0.001
Cbl-b/CD8	Low/high	105/106	65.6/18.8	191.2/21.6	3.282	2.213	4.868	<0.001	2.374	1.565	3.602	<0.001	3.325	1.631	6.779	0.001
Cbl-b/CD4	Low/high	105/106	65.2/22.5	NR/21.2	3.080	2.088	4.544	<0.001	2.675	1.723	4.153	<0.001	3.325	1.631	6.779	0.001

Number, OS, and DFS in subgroups categorized by the status of BTLA/CD8 and Cbl-b/CD8

Combined variables	n	5-year survival, %	Median survival time, months	Median disease-free survival time, months
BTLA/CD8 ^{high} and Cbl-b/CD8 ^{high}	80	17.1	20.8	15.2
BTLA/CD8 ^{high} and Cbl-b/CD8 ^{low}	26	31.3	18.7	14.2
BTLA/CD8 ^{low} and Cbl-b/CD8 ^{high}	25	31.2	27.1	19.9
BTLA/CD8 ^{low} and Cbl-b/CD8 ^{low}	80	78.3	NR	NR

Density ratios are shown of FOXP3 to CD4 (FOXP3/CD4), B and T lymphocyte attenuator (BTLA) to CD8 (BTLA/CD8), BTLA to CD4 (BTLA/CD4), Casitas-B-lineage lymphoma protein-b (Cbl-b) to CD8 (Cbl-b/CD8), and Cbl-b to CD4 (Cbl-b/CD4). C, cystic duct; CI, confidence interval; F, female; Gb, gallbladder body; Gf, gallbladder fundus; Gn, gallbladder neck; HR, hazard ratio; L, lymphatic invasion; M, male; NR, not reached; Pn, perineural invasion; V, venous invasion. Bold values, P < 0.05.

BTLA/CD8 ratio was significantly associated with shorter DFS and OS. These findings suggest that BTLA is involved in the formation of a protumor microenvironment, supporting the contention that BTLA is an important co-inhibitory molecule in the orchestration of immunosuppressive networks in cancer, and therefore a potential new target for interventions aimed at reversal of immune evasion and boosting of antitumor immunity in cancer patients.

It has been shown that BTLA binds to the herpes virus entry mediator (HVEM),⁽⁴³⁾ inhibits T-cell proliferation and cytokine production *in vitro*, and mediates the negative regulation of CD8⁺ T-cell homeostasis and memory cell generation *in vivo*.⁽⁴⁴⁾ In the context of cancer immunology, BTLA–HVEM is known to be another inhibitory pathway used by cancer cells to impair the antitumor immune response.^(45–47) HVEM is constitutively expressed on naive T cells and downregulated following T cell activation, only to be re-expressed later on effector and memory T cells.⁽⁴⁸⁾ It is also broadly expressed on cells of the immune system such as Tregs, B cells, monocytes, neutrophils, NK cells, and DCs, in addition to epithelial cells.^(49,50) Although it would have been informative to examine the distribution of HVEM immunohistochemically, we were unable to do so, because of the lack of reliable antibody specific for HVEM. In contrast to the CTLA-4 and PD-1 pathways, HVEM binds to several receptor molecules, generating immune-positive and -negative signals according to the receptors involved. Therefore, the total expression of BTLA in the tumor microenvironment might be a simpler and more accurate indicator of the protumor microenvironment, rather than expression of HVEM. It remains to be investigated whether a specific cell type with high BTLA expression exerts a predominantly inhibitory action or whether various types of immune cells function in a coordinated manner.

Maintenance of tolerance and induction of T cell anergy is critical for prevention of autoimmunity. However, in cases of malignancy, tumor-induced T cell anergy and/or tolerance induces cancer-associated immune paralysis, which contributes, at least in part, to uncontrolled tumor growth and metastasis. No previous studies have, in fact, demonstrated anergy cells in tissues. In the present study, we observed that T cells that had infiltrated and become attached to cancer cells were often positive for Cbl-b, and sometimes positive for BTLA. Although no BTLA⁺Cbl-b⁺ cells were found, T cells that had infiltrated within cancer nests were suggested to have become anergic under the influence of BTLA signals. Our clinicopathological analyses revealed that Cbl-b/CD8 was increased in GBC relative to CC and XGC, and that Cbl-b/CD8 in tumor-infiltrating immune cells was higher in patients with more advanced cancer, as was the case for BTLA expression. Moreover, Cbl-b/CD8 was significantly and positively correlated with BTLA/CD8 and FOXP3/CD4, and a higher Cbl-b/CD8 ratio was an independent indicator of poor prognosis in terms of DFS and OS for patients with GBC. Accordingly, it is suggested that T cell anergy in the tumor microenvironment, reflected by the

expression of Cbl-b, represents promotion of a protumor microenvironment in GBC, in concert with BTLA. In addition, Cbl-b expression may be a useful marker for evaluating T cell anergy in the tumor microenvironment. Here we have shown for the first time the usefulness of Cbl-b for evaluation of the tumor microenvironment.

Therapeutic blockade of the immune checkpoint pathways, CTLA-4 and PD-1/PD-L1, has shown promise in a variety of malignancies,^(23,51) although the effectiveness of the reagents used, especially anti-CTLA4 antibody, has been rather limited for major epithelial cancers in comparison with melanoma, and even in melanoma cases showing basic or acquired resistance have often been observed. In addition, a wide range of immune-related adverse events have also been observed following treatment.^(23,51) To increase the antitumor effect and to reduce the incidence of immune-related adverse events, optimization of the dose and schedule of reagents, and characterization of biomarkers associated with disease outcome, have been extensively investigated. In addition, various combination approaches have been considered, including blockade of immune checkpoints together with the use of other anticancer treatments such as chemotherapy, radiotherapy, targeted therapy, and other forms of immunotherapy. Some combination approaches have achieved enhanced antitumor effects in animal models and human clinical studies,^(29–31) in which monotherapy has exerted only modest effects. Novel immune checkpoints are currently being investigated based on experience with CTLA-4 and PD-1/PD-L1. Various combination approaches using these novel checkpoints may yield a therapeutic edge in the battle against a range of cancers. Therefore, it is suggested that our data for BTLA in GBC will be useful for future studies aimed at developing this new approach.

In conclusion, our findings suggest that BTLA in the tumor microenvironment plays an inhibitory role in the immune reaction against GBC, in concert with other factors. Higher expression of BTLA and Cbl-b in tumor-infiltrating immune cells appears to be an indicator of poor prognosis, whereas a higher ratio of non-anergic CD8⁺ T cells is an independent favorable prognostic factor in GBC patients. Targeting BTLA for reversal of immune evasion may represent a promising new therapeutic approach.

Acknowledgments

This work was supported by a Grant-in-Aid for Scientific Research from the Ministry of Education, Culture, Sports, Science and Technology of Japan (N.H.), and the National Cancer Center Research and Development Fund (N.H.). The authors thank Ms. Keiko Gomisawa for excellent technical assistance.

Disclosure Statement

The authors have no conflict of interest.

References

- 1 Reid KM, Ramos-De la Medina A, Donohue JH. Diagnosis and surgical management of gallbladder cancer: a review. *J Gastrointest Surg* 2007; **11**: 671–81.
- 2 D'Angelica M, Dalal KM, DeMatteo RP, Fong Y, Blumgart LH, Jarnagin WR. Analysis of the extent of resection for adenocarcinoma of the gallbladder. *Ann Surg Oncol* 2009; **16**: 806–16.
- 3 Hueman MT, Vollmer CM Jr, Pawlik TM. Evolving treatment strategies for gallbladder cancer. *Ann Surg Oncol* 2009; **16**: 2101–15.
- 4 Gourgoutis S, Kocher HM, Solaini L, Yarollahi A, Tsiambas E, Salemis NS. Gallbladder cancer. *Am J Surg* 2008; **196**: 252–64.
- 5 Shukla PJ, Neve R, Barreto SG *et al*. A new scoring system for gallbladder cancer (aiding treatment algorithm): an analysis of 335 patients. *Ann Surg Oncol* 2008; **15**: 3132–7.
- 6 Vesely MD, Kershaw MH, Schreiber RD, Smyth MJ. Natural innate and adaptive immunity to cancer. *Annu Rev Immunol* 2011; **29**: 235–71.
- 7 Poschke I, Mougiakakos D, Kiessling R. Camouflage and sabotage: tumor escape from the immune system. *Cancer Immunol Immunother* 2011; **60**: 1161–71.

- 8 Rabinovich GA, Gabrilovich D, Sotomayor EM. Immunosuppressive strategies that are mediated by tumor cells. *Annu Rev Immunol* 2007; **25**: 267–96.
- 9 Zou W. Immunosuppressive networks in the tumour environment and their therapeutic relevance. *Nat Rev Cancer* 2005; **5**: 263–74.
- 10 Naito Y, Saito K, Shiiba K *et al*. CD8+ T cells infiltrated within cancer cell nests as a prognostic factor in human colorectal cancer. *Cancer Res* 1998; **58**: 3491–4.
- 11 Pages F, Berger A, Camus M *et al*. Effector memory T cells, early metastasis, and survival in colorectal cancer. *N Engl J Med* 2005; **353**: 2654–66.
- 12 Zhang L, Conejo-Garcia JR, Katsaros D *et al*. Intratumoral T cells, recurrence, and survival in epithelial ovarian cancer. *N Engl J Med* 2003; **348**: 203–13.
- 13 Schumacher K, Haensch W, Roefzaad C, Schlag PM. Prognostic significance of activated CD8(+) T cell infiltrations within esophageal carcinomas. *Cancer Res* 2001; **61**: 3932–6.
- 14 Wada Y, Nakashima O, Kutami R, Yamamoto O, Kojiro M. Clinicopathological study on hepatocellular carcinoma with lymphocytic infiltration. *Hepatology* 1998; **27**: 407–14.
- 15 Hiraoka N, Ino Y, Yamazaki-Itoh R, Kanai Y, Kosuge T, Shimada K. Intratumoral tertiary lymphoid organ is a favourable prognosticator in patients with pancreatic cancer. *Br J Cancer* 2015; **112**: 1782–90.
- 16 Ino Y, Yamazaki-Itoh R, Shimada K *et al*. Immune cell infiltration as an indicator of the immune microenvironment of pancreatic cancer. *Br J Cancer* 2013; **108**: 914–23.
- 17 Curiel TJ, Coukos G, Zou L *et al*. Specific recruitment of regulatory T cells in ovarian carcinoma fosters immune privilege and predicts reduced survival. *Nat Med* 2004; **10**: 942–9.
- 18 Hiraoka N, Onozato K, Kosuge T, Hirohashi S. Prevalence of FOXP3+ regulatory T cells increases during the progression of pancreatic ductal adenocarcinoma and its premalignant lesions. *Clin Cancer Res* 2006; **12**: 5423–34.
- 19 Kobayashi N, Hiraoka N, Yamagami W *et al*. FOXP3+ regulatory T cells affect the development and progression of hepatocarcinogenesis. *Clin Cancer Res* 2007; **13**: 902–11.
- 20 Nakakubo Y, Miyamoto M, Cho Y *et al*. Clinical significance of immune cell infiltration within gallbladder cancer. *Br J Cancer* 2003; **89**: 1736–42.
- 21 Goepfert B, Frauschuh L, Zucknick M *et al*. Prognostic impact of tumour-infiltrating immune cells on biliary tract cancer. *Br J Cancer* 2013; **109**: 2665–74.
- 22 Chen L, Flies DB. Molecular mechanisms of T cell co-stimulation and co-inhibition. *Nat Rev Immunol* 2013; **13**: 227–42.
- 23 Pardoll DM. The blockade of immune checkpoints in cancer immunotherapy. *Nat Rev Cancer* 2012; **12**: 252–64.
- 24 Brahmer JR, Tykodi SS, Chow LQ *et al*. Safety and activity of anti-PD-L1 antibody in patients with advanced cancer. *N Engl J Med* 2012; **366**: 2455–65.
- 25 Hodi FS, O'Day SJ, McDermott DF *et al*. Improved survival with ipilimumab in patients with metastatic melanoma. *N Engl J Med* 2010; **363**: 711–23.
- 26 Robert C, Thomas L, Bondarenko I *et al*. Ipilimumab plus dacarbazine for previously untreated metastatic melanoma. *N Engl J Med* 2011; **364**: 2517–26.
- 27 Topalian SL, Hodi FS, Brahmer JR *et al*. Safety, activity, and immune correlates of anti-PD-1 antibody in cancer. *N Engl J Med* 2012; **366**: 2443–54.
- 28 Watanabe N, Gavrieli M, Sedy JR *et al*. BTLA is a lymphocyte inhibitory receptor with similarities to CTLA-4 and PD-1. *Nat Immunol* 2003; **4**: 670–9.
- 29 Curran MA, Montalvo W, Yagita H, Allison JP. PD-1 and CTLA-4 combination blockade expands infiltrating T cells and reduces regulatory T and myeloid cells within B16 melanoma tumors. *Proc Natl Acad Sci USA* 2010; **107**: 4275–80.
- 30 Matsuzaki J, Gnjjatic S, Mhaweck-Fauceglia P *et al*. Tumor-infiltrating NY-ESO-1-specific CD8+ T cells are negatively regulated by LAG-3 and PD-1 in human ovarian cancer. *Proc Natl Acad Sci USA* 2010; **107**: 7875–80.
- 31 Wolchok JD, Kluger H, Callahan MK *et al*. Nivolumab plus ipilimumab in advanced melanoma. *N Engl J Med* 2013; **369**: 122–33.
- 32 M'Hidi H, Thibault ML, Chetaille B *et al*. High expression of the inhibitory receptor BTLA in T-follicular helper cells and in B-cell small lymphocytic lymphoma/chronic lymphocytic leukemia. *Am J Clin Pathol* 2009; **132**: 589–96.
- 33 Feng XY, Wen XZ, Tan XJ *et al*. Ectopic expression of B and T lymphocyte attenuator in gastric cancer: a potential independent prognostic factor in patients with gastric cancer. *Mol Med Rep* 2015; **11**: 658–64.
- 34 Hurchla MA, Sedy JR, Gavrieli M, Drake CG, Murphy TL, Murphy KM. B and T lymphocyte attenuator exhibits structural and expression polymorphisms and is highly induced in anergic CD4+ T cells. *J Immunol* 2005; **174**: 3377–85.
- 35 Loeser S, Penninger JM. The ubiquitin E3 ligase Cbl-b in T cells tolerance and tumor immunity. *Cell Cycle* 2007; **6**: 2478–85.
- 36 Heissmeyer V, Macian F, Im SH *et al*. Calcineurin imposes T cell unresponsiveness through targeted proteolysis of signaling proteins. *Nat Immunol* 2004; **5**: 255–65.
- 37 Jeon MS, Atfield A, Venuprasad K *et al*. Essential role of the E3 ubiquitin ligase Cbl-b in T cell anergy induction. *Immunity* 2004; **21**: 167–77.
- 38 Albores-Saavedra J, Adsay NV, Crawford JM *et al*. Carcinoma of the gallbladder and extrahepatic ducts. In: Bosman FT, Carneiro F, Hruban RH, Theise ND, eds. *WHO Classification of Tumours of the Digestive System*, 4th edn. Lyon, France: IARC, 2010; 266–73.
- 39 Sobin LH, Gospodarowicz MK, Wittekind C. *TNM Classification of Malignant Tumors*, 7th edn. New York: Wiley-Blackwell, 2009.
- 40 Japanese Society of Biliary Surgery. *Classification of Biliary Tract Carcinoma*, 2nd edn. Tokyo, Japan: Kanehara, 2004.
- 41 Takahashi Y, Hiraoka N, Onozato K *et al*. Solid-pseudopapillary neoplasms of the pancreas in men and women: do they differ? *Virchows Arch* 2006; **448**: 561–9.
- 42 Sato E, Olson SH, Ahn J *et al*. Intraepithelial CD8+ tumor-infiltrating lymphocytes and a high CD8+/regulatory T cell ratio are associated with favorable prognosis in ovarian cancer. *Proc Natl Acad Sci USA* 2005; **102**: 18538–43.
- 43 Sedy JR, Gavrieli M, Potter KG *et al*. B and T lymphocyte attenuator regulates T cell activation through interaction with herpesvirus entry mediator. *Nat Immunol* 2005; **6**: 90–8.
- 44 Krieg C, Boyman O, Fu YX, Kaye J. B and T lymphocyte attenuator regulates CD8+ T cell-intrinsic homeostasis and memory cell generation. *Nat Immunol* 2007; **8**: 162–71.
- 45 Derre L, Rivals JP, Jandus C *et al*. BTLA mediates inhibition of human tumor-specific CD8+ T cells that can be partially reversed by vaccination. *J Clin Invest* 2010; **120**: 157–67.
- 46 Fourcade J, Sun Z, Pagliano O *et al*. CD8(+) T cells specific for tumor antigens can be rendered dysfunctional by the tumor microenvironment through upregulation of the inhibitory receptors BTLA and PD-1. *Cancer Res* 2012; **72**: 887–96.
- 47 Hobo W, Norde WJ, Schaap N *et al*. B and T lymphocyte attenuator mediates inhibition of tumor-reactive CD8+ T cells in patients after allogeneic stem cell transplantation. *J Immunol* 2012; **189**: 39–49.
- 48 del Rio ML, Lucas CL, Buhler L, Rayat G, Rodriguez-Barbosa JI. HVEM/LIGHT/BTLA/CD160 cosignaling pathways as targets for immune regulation. *J Leukoc Biol* 2010; **87**: 223–35.
- 49 Morel Y, Truneh A, Sweet RW, Olive D, Costello RT. The TNF superfamily members LIGHT and CD154 (CD40 ligand) costimulate induction of dendritic cell maturation and elicit specific CTL activity. *J Immunol* 2001; **167**: 2479–86.
- 50 Xu H, Cao D, Guo G, Ruan Z, Wu Y, Chen Y. The intrahepatic expression and distribution of BTLA and its ligand HVEM in patients with HBV-related acute-on-chronic liver failure. *Diagn Pathol* 2012; **7**: 142.
- 51 Postow MA, Callahan MK, Wolchok JD. Immune checkpoint blockade in cancer therapy. *J Clin Oncol* 2015; **33**: 1974–82.

Supporting Information

Additional supporting information may be found in the online version of this article:

Fig. S1. Comparison of infiltrating cells in gallbladder lesion.

Fig. S2. Kaplan–Meier survival curves.

Table S1. Univariate and multivariate survival analyses.